

Development of biodegradable and antimicrobial electrospun zein fibers for food packaging

Zeynep Aytac, Runze Huang, Nachiket Vaze, Tao Xu, Brian David Eitzer, Walter Krol, Luke A. MacQueen, Huibin Chang, Douglas W. Bousfield, Mary B Chan-Park, Kee Woei Ng, Kevin Kit Parker, Jason C. White, and Philip Demokritou

ACS Sustainable Chem. Eng., **Just Accepted Manuscript** • DOI: 10.1021/acssuschemeng.0c05917 • Publication Date (Web): 21 Sep 2020

Downloaded from pubs.acs.org on September 28, 2020

Just Accepted

“Just Accepted” manuscripts have been peer-reviewed and accepted for publication. They are posted online prior to technical editing, formatting for publication and author proofing. The American Chemical Society provides “Just Accepted” as a service to the research community to expedite the dissemination of scientific material as soon as possible after acceptance. “Just Accepted” manuscripts appear in full in PDF format accompanied by an HTML abstract. “Just Accepted” manuscripts have been fully peer reviewed, but should not be considered the official version of record. They are citable by the Digital Object Identifier (DOI®). “Just Accepted” is an optional service offered to authors. Therefore, the “Just Accepted” Web site may not include all articles that will be published in the journal. After a manuscript is technically edited and formatted, it will be removed from the “Just Accepted” Web site and published as an ASAP article. Note that technical editing may introduce minor changes to the manuscript text and/or graphics which could affect content, and all legal disclaimers and ethical guidelines that apply to the journal pertain. ACS cannot be held responsible for errors or consequences arising from the use of information contained in these “Just Accepted” manuscripts.

1 2 3 4 5 6 7 8 9 10 11 12 13 14 15 16 17 18 19 20 21 22 23 24 25 26 27 28 29 30 31 32 33 34 35 36 37 38 39 40 41 42 43 44 45 46 47 48 49 50 51 52 53 54 55 56 57 58 59 60

1 2 3 4 5 6 7 8 9 10 11 12 13 14 15 16 17 18 19 20 21 22 23 24 25 26 27 28 29 30 31 32 33 34 35 36 37 38 39 40 41 42 43 44 45 46 47 48 49 50 51 52 53 54 55 56 57 58 59 60

1 2 3 4 5 6 7 8 9 10 11 12 13 14 15 16 17 18 19 20 21 22 23 24 25 26 27 28 29 30 31 32 33 34 35 36 37 38 39 40 41 42 43 44 45 46 47 48 49 50 51 52 53 54 55 56 57 58 59 60

Zeynep Aytac^a, Runze Huang^a, Nachiket Vaze^a, Tao Xu^a, Brian David Eitzer^b, Walter Krol^b,
Luke A. MacQueen^c, Huibin Chang^c, Douglas W. Bousfield^d, Mary B. Chan-Park^e, Kee Woei
Ng^{a,f,g}, Kevin Kit Parker^c, Jason C. White^b, Philip Demokritou^{a,f*}

^a Center for Nanotechnology and Nanotoxicology, Department of Environmental Health, Harvard
T. H. Chan School of Public Health, Harvard University, 665 Huntington Avenue, Boston, MA,
02115, USA

^b Department of Analytical Chemistry, The Connecticut Agricultural Experiment Station, 123
Huntington Street, New Haven, CT, 06504, USA

^c Disease Biophysics Group, John A. Paulson School of Engineering and Applied Sciences,
Harvard University, 29 Oxford Street, Pierce Hall 318, Cambridge, MA, 02138, USA

^d Department of Chemical and Biological Engineering, University of Maine, Orono, Maine,
04469, United States

^e School of Chemical and Biomedical Engineering, Nanyang Technological University, 62
Nanyang Drive, Singapore 637459, Singapore

^f School of Materials Science and Engineering, Nanyang Technological University, 50 Nanyang
Avenue, 639798, Singapore

^g Environmental Chemistry and Materials Centre, Nanyang Environment and Water Research
Institute, 1 Cleantech Loop, 637141, Singapore

* Corresponding author: Philip Demokritou, E-mail: pdemokri@hsph.harvard.edu

ABSTRACT

There is an urgent need to develop biodegradable and non-toxic materials from biopolymers and nature-derived antimicrobials to enhance food safety and quality. In this study, electrospinning was used as a one-step, scalable, green synthesis approach to engineer antimicrobial fibers from zein using non-toxic organic solvents and a cocktail of nature-derived antimicrobials which are all FDA-classified Generally Recognized as Safe (GRAS) for food use. Morphological and physicochemical properties of fibers, as well as the dissolution kinetics of antimicrobials were assessed along with their antimicrobial efficacy using state of the art analytical and microbiological methods. A cocktail of nature-derived antimicrobials was developed and included thyme oil, citric acid, and nisin. Its ability to inactivate a broad-spectrum of with food-related pathogens was demonstrated.

1
2
3 32 Morphological characterization of the electrospun antimicrobial fibers revealed bead-free fibers
4
5 33 with a small average diameter of 165 nm, whereas physicochemical characterization showed high
6
7 34 surface area-to-volume ratio (specific surface area:21.91 m²/g) and presence of antimicrobial
8
9
10 35 analytes in the fibers. The antimicrobials exhibited initial rapid release from the fibers in 2 hours
11
12 36 into various food simulants. Furthermore, the antimicrobial fibers effectively reduced *E. coli* and
13
14 37 *L. innocua* populations by ~5 logs for after 24-hours and 1-hour of exposure, respectively. More
15
16
17 38 importantly, due to the small diameter and high surface area-to-volume ratio of the fibers, only
18
19 39 miniscule quantities of fiber mass and antimicrobials per surface area (2.50 mg/cm² of fibers) are
20
21 40 needed for pathogen inactivation. The scalability of this fiber synthesis process was also
22
23 41 demonstrated using a multi-needle injector with production yield up to 1 g/h. This study shows the
24
25
26 42 potential of using nature-derived biopolymers and antimicrobials to synthesize fibers for
27
28 43 sustainable food packaging materials.

30
31 44
32
33 45 **Keywords:** electrospinning, sustainable food packaging, biopolymers, zein, food safety and quality
34

35 46

37 47

39 48

41 49

43 50

45 51

47 52

49 53

51 54

55 INTRODUCTION

56 The global population is expected to reach 10 billion by 2050, and there is an urgent need
57 to find ways to provide the global populace with safe and nutritious food, while at the same time
58 minimizing the significant impact of agriculture on the environment.^{1,2,3} The globalization of the
59 food supply has also introduced major challenges associated with food safety and quality. The
60 WHO estimates that microbial contamination causes 584 million foodborne illnesses and 347,000
61 deaths annually around the world.² The monetary loss caused by foodborne illness in the US is
62 estimated to be more than 15.5 billion dollars per year.⁴ In addition, it is estimated that 30-40% of
63 the food supply is wasted in the US due to the presence of spoilage microorganisms.⁵

64 One of the most efficient ways to prevent foodborne disease outbreaks and reduce food
65 spoilage and waste is to develop efficient food packaging materials, as food products spend a
66 considerable amount of time inside packaging while in transit from the farm to the fork.⁶ Currently,
67 the majority of packaging is passive, providing only an inert barrier to the external environment.⁷
68 More importantly, the concept of active or intelligent packaging has emerged. These types of
69 packaging aim to extend the shelf life and improve safety and quality of food, not only by protecting
70 the contents from degradation due to oxygen, water vapor, etc., but also by incorporating sensing
71 and other antimicrobial approaches.⁸

72 Synthetic, petroleum-based polymers such as polyethylene terephthalate (PET),
73 polyethylene (PE), polypropylene (PP), and polystyrene (PS) are widely used as a film for food
74 packaging due to their low cost and useful mechanical and gas barrier properties.⁹ However, the
75 use of synthetic non-biodegradable polymers in food packaging and beyond has led to the so-called
76 “micro-nano plastics crisis”, which is an emerging issue of major environmental health concern.¹⁰
77 More importantly, the recycling rate of these polymeric films is quite low.¹¹ More, recently, interest

1
2
3 78 has increased significantly in the use of biodegradable biopolymers for sustainable food packaging
4
5 79 applications.¹² Such materials include polymeric films made of natural polymers such as starch,
6
7 80 zein, and gelatin; polymers synthesized by bacterial fermentation such as polyhydroxy butyrate
8
9 81 (PHB) and polyhydroxy butyrate-valerate (PHBV); and polymers synthesized from nature-derived
10
11 82 monomers such as polylactic acid (PLA).¹²
12
13

14 83 An emerging approach for producing antimicrobial active packaging materials is the use of
15
16 84 polymer films made of inherently antimicrobial materials such as ϵ -polylysine and chitosan.¹³
17
18 85 However, the antimicrobial activity achieved with these materials is often not adequate.¹⁴ Another
19
20 86 approach is the incorporation of antimicrobial agents into the films.¹⁵ However, the main issue of
21
22 87 the film-based materials is the low surface-to-volume ratio which requires high quantities of
23
24 88 antimicrobial agents for achieving satisfactory antimicrobial effects. This may result in negative
25
26 89 sensory effects on the food, such as smell, discoloration, etc.¹⁶
27
28
29

30 90 More recently, nanotechnology has emerged as a promising avenue for the development of
31
32 91 novel advanced bio-degradable food packaging materials to enhance food safety and quality.^{17,18}
33
34 92 For example, nanocellulose-based films have been explored due to their excellent gas barrier
35
36 93 properties.¹⁹ Furthermore, electrospun fibers synthesized from both synthetic polymers and
37
38 94 biopolymers (e.g. polylactic acid, zein, amaranth, and pullulan) were infused with antimicrobial
39
40 95 agents, including carvacrol, thymol, and nisin, to be used for food package materials.^{20,21,22} In the
41
42 96 study of Altan et al., carvacrol was incorporated into electrospun zein and PLA nanofibers for
43
44 97 extending the shelf life of whole wheat bread.²⁰ Similarly, active food packaging materials for
45
46 98 prolonging shelf life of meat was developed from electrospun zein nanofibers incorporated with
47
48 99 the cyclodextrin-inclusion complex of thymol by Aytac et al.²¹ Soto et al. reported the synthesis of
49
50 100 nisin-loaded amaranth protein isolate:pullulan (API:PUL) nanofibers to be used for apple juice and
51
52
53
54
55

1
2
3 101 fresh cheese package.²² Such fibers can be used to coat widely used polymer-based food packaging
4
5 102 materials and provide antimicrobial functionality. The most important advantage of fibers over
6
7 103 polymeric films is their high surface-to-volume ratio. This enables almost all antimicrobial agents
8
9
10 104 to be on the surface, especially if the diameter of fibers is in the nanoscale (< 100 nm). However,
11
12 105 synthesis of most electrospun fibers used in food packaging materials is not “green” since harsh
13
14 106 organic solvents are typically used, and high quantity of essential oils per surface area are widely
15
16
17 107 used to provide satisfactory and broad antimicrobial efficacy which may cause negative effects on
18
19 108 the organoleptic properties of food. It is also worth noting that a big challenge of electrospinning
20
21 109 is the scalability. However, recent advancements on electrospinning and development of automated
22
23
24 110 multi-injector designs make it possible to increase the production yields.²³ As shown in previous
25
26 111 studies by the authors and others, using a cocktail of antimicrobial active ingredients (AIs) rather
27
28 112 than a single analyte enhances antimicrobial activity across a spectrum of microorganisms due to
29
30
31 113 synergistic effects.^{24,25}

32
33 114 In this study, electrospinning was used as a one-step synthesis approach to engineer
34
35 115 functional fibers from zein using non-toxic organic solvents. Zein was selected to synthesize fibers
36
37 116 since it is an amphiphilic, edible, bio-degradable, and Generally Regarded as Safe (GRAS)
38
39
40 117 biopolymer by US FDA. A cocktail of nature-derived and US FDA approved as GRAS
41
42 118 antimicrobial AIs was explored and antimicrobial activity against a broad spectrum of food
43
44
45 119 pathogens was assessed by microbiological assays. The antimicrobials were incorporated into the
46
47 120 chemical structure of the fibers using a direct solution integration method. The morphological and
48
49 121 physicochemical properties of fibers, and AI dissolution kinetics as a function of time were
50
51 122 assessed, along with their antimicrobial efficacy using a broad range of analytical and
52
53
54 123 microbiological methods.

124 METHODS

125 **“Green” synthesis of zein fibers using electrospinning:** Figure 1a-b illustrates the one-
126 step, green synthesis of fibers using electrospinning. The electrospinning apparatus (DOXA
127 Microfluidics, Málaga, Spain) consists of four main components: syringe pump, injector, high
128 voltage power supply, and collector. When high voltage is applied to a polymer solution, it is
129 electrified. The so-called “Taylor cone” is then formed at the tip of the injector due to the distortion
130 of the drop of polymer solution under the electric field. Once the electric field is high enough to
131 overcome the surface tension of the polymer solution, a jet is formed and moved towards the
132 collector. As the solvent evaporates, fibers are deposited on the collector/substrate.²⁶ The
133 electrospinning parameters such as flow rate, applied voltage, and needle-collector distance can be
134 modified in order to optimize the morphology and other properties of the fibers.²⁶

135 Synthesis of pristine zein fibers (ZF): Zein (zein from maize, Sigma Aldrich, Z3625)
136 solutions of various concentrations were prepared in acetic acid for synthesizing pristine zein fibers
137 (ZF) in order to assess the effect of zein concentration on fiber morphology and to identify
138 concentration for bead-free electrospun fibers. The zein solutions were then loaded in a plastic
139 syringe (10 mL BD Luer-Lock™ tip) and a syringe pump was used to supply the solution through
140 a stainless-steel single-needle injector (diameter:0.6 mm, 90° blunt end). Voltage was applied from
141 the high voltage power supply to both the needle tip and collector. The electrospinning parameters
142 such as flow rate, applied voltage, and needle-collector distance were modified along with zein
143 concentrations to obtain bead-free zein fibers. ZF were randomly deposited on traditional food
144 package substrates such as aluminum foil (20×20 cm²) or cellulose nanofibril (CNF) film^{27,28}
145 (diameter:10 cm). By varying the collection time, the mass of the fibers per surface area can be
146 adjusted.

1
2
3 147 Synthesis of antimicrobial zein fibers (AZF): The antimicrobial cocktail, composed of the
4
5 148 active ingredients (AIs) selected as described below, was incorporated into zein solution using a
6
7 149 direct solution integration method and was then used for the synthesis of fibers by electrospinning.
8
9
10 150 In summary, the cocktail was dissolved in acetic acid and zein was then added into the solution,
11
12 151 followed by stirring until complete dissolution was achieved. The solution was then loaded into a
13
14 152 plastic syringe (10 mL BD Luer-Lock™ tip) and other electrospinning parameters including flow
15
16 153 rate, applied voltage, and needle-collector distance were systematically modified to obtain bead
17
18 154 free AZFs as described above for the case of pristine ZFs. AZFs were randomly deposited on
19
20 155 traditional food package substrates as above.
21
22

23
24 156 **Morphological characterization of zein fibers**: Morphological characterization of the
25
26 157 fibers was performed using scanning electron microscopy (SEM, Zeiss FESEM Ultra Plus). For
27
28 158 this purpose, the fibers were peeled off from the substrate and cut into small pieces. The piece of
29
30 159 fiber sample was then mounted on a stub using double-sided carbon tape and images were taken.
31
32
33 160 The average diameter of the fibers was calculated from SEM images using Image J Software
34
35 161 (n=100) and the results are reported as average \pm standard deviation.
36
37

38 162 **Physicochemical characterization of zein fibers**: The fiber specific surface area (m^2/g),
39
40 163 fiber average pore diameter (nm), and total pore volume (cc/g) of the fibers were measured using
41
42 164 a Brunauer-Emmett-Teller (BET, Quantachrome NOVA touch LX4) surface area analyzer. Low
43
44 165 temperature (77.35 K) nitrogen adsorption isotherms were measured at relative pressures from
45
46 166 0.005 to 1.00. Prior to measurement, fibers were degassed in 9 mm cell at 323.15 K for 24 hours.
47
48

49 167 The crystallinity of nisin and the fibers were investigated with $\text{Cu K}\alpha$ radiation by and X-
50
51 168 ray diffraction (XRD, Bruker D2 Phaser) in the 2θ range of 10° - 100° . XRD could not be performed
52
53 169 for thyme oil and citric acid due to their liquid state at room temperature.
54
55

1
2
3 170 Chemical characterization of AIs and fibers was performed by Fourier transform infrared
4
5 171 spectrometry (ATR-FTIR). The infrared spectra of AIs and fibers were obtained by an ATR-FTIR
6
7 172 (Thermo Scientific Nicolet IS50). The spectra were recorded between 4000 cm^{-1} and 400 cm^{-1} at
8
9
10 173 the resolution of 4 cm^{-1} and 64 scans were taken per sample.

11
12 174 **Development of antimicrobial active ingredient (AI) cocktail:** In order to determine the
13
14 175 AI cocktail to be used, we examined the antimicrobial efficacy of a range of concentrations of
15
16 176 various nature-derived antimicrobials including essential oils, organic acids, peptides²⁹ and their
17
18 177 combinations. This includes thyme oil, citric acid, and nisin. Essential oils are a group of volatile
19
20 178 compounds extracted from plants; are effective growth inhibitors against bacteria, fungi, and
21
22 179 viruses; and have been studied as antimicrobial agents in food packaging.^{30,31} Among essential oils,
23
24 180 thyme oil is found to be one of the most effective compounds.³² Organic acids exhibit their
25
26 181 antimicrobial effect by damaging the bacterial membrane and causing stress on intracellular pH
27
28 182 homeostasis.^{33,34} Citric acid, commonly found in citrus fruits, shows inhibition effect against
29
30 183 foodborne pathogens such as *Escherichia coli*, *Listeria monocytogenes*, and *Salmonella*.^{35,36}
31
32 184 Bacteriocins are antimicrobial peptides showing their effect while inducing permeabilization by
33
34 185 disrupting the bacterial membrane or moving across the membrane and interacting with internal
35
36 186 targets (i.e. DNA), ultimately killing the cell.³⁷ Nisin, which is very effective bacteriocin, can
37
38 187 inhibit the growth of various gram-positive bacteria, including *Listeria monocytogenes*,
39
40 188 *Clostridium botulinum*, and *Staphylococcus aureus*.³²

41
42 189 The antimicrobial efficacy of AIs against known food pathogen surrogates, *Escherichia coli*
43
44 190 (*E. coli*) ATCC#25922 and *Listeria innocua* (*L. innocua*) ATCC#33090, was assessed using the
45
46 191 disk diffusion test described in detail by Hudzicki et al.³⁸ as follows:
47
48
49
50
51
52
53
54
55
56
57
58
59
60

1
2
3 192 Inoculum preparation: To prepare the inoculum of *E. coli* and *L. innocua* for the disk
4
5 193 diffusion test, a single colony was selected, transferred into 30 mL of tryptic soy broth (TSB; Hardy
6
7 194 Diagnostic, Santa Maria, CA) and incubated at 37°C for 18-24 hours. The culture was then
8
9
10 195 centrifuged at $\sim 2056\times g$ for 20 minutes, and the supernatant was discarded. The culture pellet was
11
12 196 resuspended in phosphate buffered saline (PBS; Hardy Diagnostic, Santa Maria, CA), and the
13
14 197 concentration was adjusted to $\sim 10^8$ CFU/mL using O.D.600 measurement with a UV/Vis
15
16
17 198 spectrophotometer (Beckman Coulter, Brea, CA).

19 199 Consequently, dispersion of single AIs and their combinations were prepared fresh in sterile
20
21 200 deionized water. It is worth noting that the antimicrobial activity of 0.005% (w/v) nisin could not
22
23 201 be investigated following the established antimicrobial assessment protocol which requires
24
25 202 dissolution in water since nisin has low solubility at neutral pH. Instead, nisin was dissolved with
26
27 203 1% (w/v) citric acid, which is the minimum amount of citric acid used in the combined AIs and its
28
29 204 efficacy assessed following the protocol described below. A positive control of 0.5 mg/mL of
30
31 205 ampicillin (VWR, Radnor, PA) and a negative control of deionized water were included. Then, 20
32
33 206 μL of each AI dispersion was added to a blank paper disk (6 mm; Hardy Diagnostic, Santa Maria,
34
35 207 CA). *E. coli* or *L. innocua* were then inoculated onto Mueller Hinton Agar (MHA; Hardy
36
37 208 Diagnostic, Santa Maria, CA) with a cotton swab. The disks impregnated with AI solutions were
38
39 209 placed onto the inoculated MHA plates. The plates were then incubated at 37°C for 24 hours, and
40
41 210 the diameter of inhibition zone was measured.

42
43
44
45
46 211 **Assessment of antimicrobial efficacy of zein fibers:** The antimicrobial efficacy of AZF
47
48 212 synthesized as described above was determined against two foodborne pathogen surrogates, *E. coli*
49
50 213 and *L. innocua*, and a spoilage-associated fungus (*Penicillium italicum* (*P. italicum*) ATCC#48144)
51
52 214 by the direct contact assay based on an ASTM protocol.³⁹ In more detail:
53
54
55

1
2
3 215 The inoculum of *E. coli* and *L. innocua* was prepared as described above. To prepare the
4
5 216 inoculum of *P. italicum* spores, a published protocol was used with slight modifications.⁴⁰ In brief,
6
7 217 *P. italicum* was inoculated onto potato dextrose agar (PDA) slants and incubated at 24°C for 7
8
9 218 days. To harvest the *P. italicum* spores, each slant was added with 2 mL of 0.01% Tween-80
10
11 219 aqueous solution, and vortexed for 30 seconds. The solution was then filtered through a two-layer
12
13 220 sterile cheese cloth, and the concentration was adjusted to $\sim 10^7$ CFU/mL with PBS using manual
14
15 221 counting with a hemocytometer (Diagnocine, Hackensack, NJ).
16
17
18

19 222 Direct contact assay: The fibers deposited on the aluminum foil substrate were cut into
20
21 223 pieces (2×2 cm²) and disinfected by ultraviolet light in a biosafety hood for 15 minutes on each
22
23 224 side and were then placed into 6-well plates. An agar slurry (0.3% agar) and 0.85% sodium chloride)
24
25 225 was prepared, autoclaved, and cooled to 45°C. The microorganism inoculum (1 mL) was then
26
27 226 added into 100 mL of agar slurry. The inoculated agar slurry (300 μ L) were then added onto each
28
29 227 test sample to form a thin layer of < 1 mm. The plates were then kept in an incubator for 0 hour
30
31 228 (control), 1 hour, and 24 hours. The relative humidity was monitored and maintained at > 75% with
32
33 229 an open tray of water. The temperature was maintained at 37°C (for *E. coli* and *L. innocua*) or 24°C
34
35 230 (for *P. italicum*). Each sample was mixed with 10 mL of PBS in a sterile 59-mL stomacher bag and
36
37 231 homogenized with a stomacher for 2 min. The elute was then serially diluted and plated onto tryptic
38
39 232 soy agar (for *E. coli* and *L. innocua*) or PDA (for *P. italicum*). Plates were incubated at 37°C for
40
41 233 24 hours (for *E. coli* and *L. innocua*) or 24°C for 5 days (for *P. italicum*). Typical colonies of
42
43 234 microorganisms were counted, and log reduction of microorganisms was calculated by comparing
44
45 235 to 0-hour control samples.
46
47
48
49
50

51 236 Controls and comparator materials: Antimicrobial efficacy of the substrate used to deposit
52
53 237 the fibers (aluminum foil), ZF, and comparator samples (aluminum foil coated with AI cocktail)
54
55

1
2
3 238 were also assessed following the direct contact assay described above. The comparator sample was
4
5 239 prepared by pipetting AI cocktail solution to uniformly cover the surface of the aluminum foil
6
7 240 having the same surface area with the substrate employed to deposit the fibers (20×20 cm²). The
8
9 241 AI cocktail solution, which consists of 1% (w/v) thyme oil, 5% (w/v) citric acid, 0.2% nisin mixture
10
11 242 (w/v, 0.005% pure nisin), was also the same in terms of composition (except zein) and the volume
12
13 243 used to prepare the fibers. Finally, the comparator sample was kept in hood for 24 hours to
14
15 244 evaporate acetic acid; the sample was then cut into 2×2 cm² pieces and weighed. The mass per
16
17 245 surface area of the samples were found to be 3.63 mg/cm² by dividing the total mass of the solution
18
19 246 on the foil by the surface area of the samples (2×2 cm²); the AI loading of the samples was also
20
21 247 calculated at 3.63 mg of AI/cm² since they were composed of 100% AIs.
22
23
24
25

26 248 Antimicrobial efficacy of the fibers at various fiber mass per surface area: The antimicrobial
27
28 249 efficacy of AZF at two mass per surface area ratios of 1.25 and 2.50 mg/cm² was assessed.
29
30

31 250 Antimicrobial efficacy of fibers over time: The antimicrobial efficacy of AZF after storage
32
33 251 at 4°C for 4 weeks was also assessed as described above to determine any shelf life effects.
34

35 252 **AI release kinetics from zein fibers in various food simulants:** The release kinetics of
36
37 253 AIs from 6.45 cm² of AZF (15 mg) were investigated by immersing fibers into 10 mL of food
38
39 254 simulant and the solutions were stirred at room temperature for 10 days.⁴¹ Water, 3% acetic acid,
40
41 255 and 50% ethanol were used as food simulants to represent aqueous non-acidic, aqueous acidic, and
42
43 256 fatty food, respectively.⁴¹ Aliquot samples (1 mL) were withdrawn from the solutions at 0, 2, 6, 12,
44
45 257 24, and 240 hours and replaced with 1 mL of fresh food simulant. The samples were filtered prior
46
47 258 to analysis, and the amount of AIs (thymol and nisin) released was selectively measured using
48
49 259 liquid chromatography/high resolution mass spectrometry (LC/HRMS, Dionex Ultimate 3000 LC
50
51 260 interfaced to a Thermo Q-exactive HRMS). Thymol was chosen among the various components of
52
53
54
55

1
2
3 261 thyme oil since it was the major component that was detected by LC/HRMS. Nisin release can be
4
5 262 detected up to 24 hours and this might be likely due to the inactivation of nisin over time.⁴² In
6
7 263 addition, nisin release in 50% ethanol was not given because 50% ethanol created a matrix effect
8
9 264 that greatly altered nisin detection, and reliable quantitation was not possible.

10
11
12 265 The LC employed an Agilent SB-C18 2.1 x 150 column with a gradient elution. Mobile
13
14 266 phase A was water with 0.1% formic acid and mobile phase B was acetonitrile with 0.1% formic
15
16 267 acid. The LC was held at 5% B for two min, then linearly increased to 95% B for 10 min, where it
17
18 268 was held for 3 minutes before returning to 5% B for 3 minutes re-equilibration. The mass
19
20 269 spectrometer was operated in the positive ESI mode at 3.5 kV with the capillary and auxiliary gas
21
22 270 temperatures set to 300°C, and the gas flows were: sheath 50, auxiliary 15, and sweep 10. The full
23
24 271 scan was set to monitor $m/z = 120-900$ at a resolution of 70,000. Nisin was monitored using the six
25
26 272 most intense ions of the cluster created by the $(M+5H)^{+5}$ cluster while thymol used the $(M+H)^{+}$ ion.
27
28
29 273 Quantitation was performed using a series of calibration standards.

30
31
32
33 274 The loading efficiency (LE) is defined as the percentage of AI that is loaded in the
34
35 275 nanofibers. LE of AIs in AZF was determined by dissolving fiber samples (15 mg) in 10 mL of
36
37 276 acetic acid. The solutions were then filtered, and measurements were performed by LC/HRMS as
38
39 277 described above. LE is calculated by using the following equation:

40
41
42 278
$$LE (\%) = (\text{concentration of the loaded AI}) / (\text{concentration of the total AI}) * 100 \text{ (Equation 1)}$$

43
44 279 The area of each AI peak was first converted to concentration (ppm) using standard
45
46 280 calibration curves and then cumulative release (%) was calculated by considering calculated LE for
47
48 281 each AI. The release experiments were carried out in triplicate, and the results were reported as
49
50 282 average \pm standard deviation.

1
2
3 283 **Scalability of fiber synthesis using a multi-needle injector:** To demonstrate the
4
5 284 scalability of the method, a 20-needle injector was used. The needles on the multi nozzle-injector
6
7 285 were arranged 10 mm apart in circular pattern with a total injector diameter of 70 mm (Figure S4a).
8
9
10 286 The solution was prepared as described above and was loaded in a plastic syringe (10 mL BD Luer-
11
12 287 Lock™ tip). While feeding the solution through a multi-nozzle injector towards the collector by a
13
14 288 syringe pump, the voltage was applied to both the needle tip and collector from high voltage power
15
16
17 289 supply. The electrospinning parameters such as flow rate, applied voltage, and needle-collector
18
19 290 distance were then systematically modified for optimization of the cone-jet stability and for the
20
21 291 synthesis of bead-free fibers. Fibers were randomly deposited on 20×20 cm² aluminum foil
22
23
24 292 substrate.

25
26 293 **Preliminary assessment of fibers affinity to attach to the substrates:** In order to improve
27
28 294 fiber affinity to the substrate surface, pressure was applied on AZF by a hydraulic press machine
29
30 295 at room temperature (Carver, Bench top standard automatic lab press, Auto Four/3012-PL, H, 30-
31
32 296 ton capacity). AZF deposited on aluminum foil (20×20 cm²) and CNF film (diameter: 10 cm) was
33
34
35 297 pressed under various pressure and time conditions. To test fiber affinity to the surface, a 200 g
36
37 298 weight was applied on fibers deposited on the aluminum foil and removed after 5 minutes. Finally,
38
39 299 the detachment of fibers from surface was visually observed to determine qualitatively fiber affinity
40
41
42 300 to the substrate.

43
44 301 **Statistical Analysis:** Three independent replicates were conducted for each antimicrobial
45
46 302 experiment. Microorganism colony counts were converted to log CFU/sample. Statistical analysis
47
48 303 was conducted using JMP (Cary, NC). A one-way analysis of variance with Tukey's multiple
49
50 304 comparison was used to identify statistically significant difference between treatments (P < 0.05).
51
52
53
54
55

1
2
3 305 The statistical analysis for AI release kinetics from zein fibers in various food simulants
4
5 306 were performed using one-way ANOVA with a Holm-Sidak multiple comparison test (Student t-
6
7
8 307 test; $p < 0.05$).

9 10 308 **RESULTS AND DISCUSSION**

11
12 309 **“Green” synthesis of zein fibers using electrospinning:** To achieve green synthesis of
13
14 310 antimicrobial electrospun fibers, the biopolymer and solvent were selected by design, as
15
16 311 demonstrated below. Zein was chosen as a biopolymer, since it is a protein-based, edible, bio-
17
18 312 degradable polymer derived from corn and is a significant byproduct of corn processing for the
19
20 313 food and bioethanol industries. Zein has been approved as GRAS by the US FDA. It has both
21
22 314 hydrophilic and hydrophobic amino acids in its structure, giving it an amphiphilic character that
23
24 315 makes it unique among biopolymers. Consequently, the presence of hydrophobic amino acids such
25
26 316 as leucine, alanine and proline in the structure eliminate the need for post treatment such as
27
28 317 crosslinking.⁴³

29
30
31
32 318 Organic solvents that are typically used in electrospinning possess a high dipole moment,
33
34 319 dielectric constant, and conductivity, as well as low surface tension. Unfortunately, most solvents
35
36 320 with these properties are quite toxic.^{44,45,46} Electrospun zein fibers have been produced by various
37
38 321 solvent mixtures, including toxic organic solvents such as dimethyl formamide.⁴⁷ Since the use of
39
40 322 toxic solvents in this study was avoided to enable a “green” synthesis strategy, acetic acid was
41
42 323 selected as the solvent. It is worth mentioning that acetic acid is an FDA approved as GRAS and
43
44 324 non-toxic compound.⁴⁸ The ability of acetic acid to dissolve both polymer and active ingredients
45
46 325 (AIs) which results in the synthesis of bead-free and homogenous zein fibers has been demonstrated
47
48 326 in our results.

1
2
3 327 Synthesis of pristine zein fibers (ZF): Bead presence is not desirable during fiber synthesis
4
5 328 because they confound fiber homogeneity and integrity. In order to synthesize bead-free zein fibers
6
7 329 (ZF), pristine zein solutions were prepared in acetic acid at concentrations ranging from 25-30%
8
9 330 (w/v) and electrospinning was then performed as described above in detail. The operational
10
11 331 parameters were systematically modified to optimize the cone-jet stability and synthesize bead free
12
13 332 fibers. After a systematic modification of each parameter, the final parameters were 0.7 mL/h, 26
14
15 333 kV (25 kV was applied to the needle, -1 kV was applied to the collector), and a 15 cm distance to
16
17 334 the collector.

21 335 **Morphological characterization of zein fibers as a function of electrospinning**
22
23 336 **parameters and zein concentration:** Bead-free pristine zein fibers (ZF) were achieved at 30%
24
25 337 (w/v) as shown in the SEM image in Figure 2a. The occurrence of bead-free fibers at this
26
27 338 concentration is due to sufficient chain entanglement and viscosity of the solution, which result in
28
29 339 strong viscoelastic forces that resist axial stretching during electrospinning.^{49,50} The fiber diameter
30
31 340 distribution graph of ZF in Figure 2b shows diameters reaching up to a maximum of 400 nm, with
32
33 341 an average diameter of 140±40 nm. As evident in Figure S1a-b-S2, bead-free fibers cannot be
34
35 342 achieved with zein solutions at 25% (w/v) and 27.5% (w/v) concentrations due to insufficient chain
36
37 343 entanglement in these solutions.

42 344 Synthesis of antimicrobial zein fibers (AZF): Zein at various concentrations in the range
43
44 345 30-37% (w/v) was directly added into the solutions of AI cocktail dissolved in acetic acid and the
45
46 346 solutions were then electrospun. In order to optimize the cone-jet stability, the operational
47
48 347 parameters such as flow rate, applied voltage, and needle-collector distance were systematically
49
50 348 modified. First, the flow rate, applied voltage, and needle-collector distance of the solution were
51
52 349 set to 0.7 mL/h, 26 kV (25 kV was applied to the needle, -1 kV was applied to the collector), and
53
54

1
2
3 350 15 cm, respectively. After adjusting the parameters, as shown in Figure 2c, the bead-free fiber
4
5 351 parameters were synthesized at zein concentration of 37% (w/v), 0.5 mL/h flow rate, 26 kV voltage
6
7 352 (25 kV was applied to the needle, -1 kV was applied to the collector), and 15 cm needle to collector
8
9 353 distance.

10
11
12 354 The fiber diameter distribution graph of bead-free AZF displayed in Figure 2d shows
13
14 355 diameters reaching up to a maximum of 400 nm, with an average diameter of 165 ± 35 nm. The
15
16 356 slight difference in the average diameters of ZF and AZF is most likely due to the increased
17
18 357 viscosity of the zein solution after AI incorporation.⁵⁰

19
20
21 358 AZFs were deposited on the substrates for 2 and 4 hours and the fibers were then weighed;
22
23 359 the masses per surface area were 1.25 mg/cm^2 and 2.50 mg/cm^2 , respectively. Since the initial
24
25 360 theoretical concentration of AIs in AZF was $\sim 10\%$, AI loading of each AZF deposited for 2 and 4
26
27 361 hours were calculated as $0.125 \text{ mg of AI/cm}^2$ and $0.250 \text{ mg of AI/cm}^2$, respectively.

28
29
30 362 **Physicochemical characterization of zein fibers:** Specific surface area (SSA), average
31
32 363 pore diameter, and total pore volume of bead-free ZF and AZF were determined by BET (Table
33
34 364 S1-S3). The multipoint BET surface area of ZF and AZF were $16.11 \text{ m}^2/\text{g}$ and $21.91 \text{ m}^2/\text{g}$,
35
36 365 respectively. It is worth noting that the SSA of AZF is a bit higher than ZF ($21.91 \text{ m}^2/\text{g}$ for AZF
37
38 366 and $16.11 \text{ m}^2/\text{g}$ for ZF). The incorporation of AIs changes the electric conductivity of the polymer
39
40 367 solution and that can result to morphology changes as shown in Figures 2a-d. In order to maintain
41
42 368 the bead free and homogenous nature of fibers slight modifications of electrospinning parameters
43
44 369 are required as presented in the results section. The average pore diameter is between 4.84 nm and
45
46 370 5.58 nm, which show that the pores in the fibers are in mesoporous range (2 and 50 nm). Total pore
47
48 371 volumes were determined to be $1.95 \times 10^{-2} \text{ cc/g}$ and $3.05 \times 10^{-2} \text{ cc/g}$ for ZF and AZF, respectively.

372 These values are consistent with the literature, in which that pore volume increases with surface
373 area.⁵¹

374 XRD was performed to determine the crystallinity of nisin, ZF, and AZF (Figure 2e). The
375 most observable nisin peaks were evident at $2\theta=31^\circ$ and $2\theta=45^\circ$, due to the characteristic
376 diffraction of sodium chloride (NaCl), which is the major component of nisin.⁵² ZF and AZF are
377 composed of an amorphous polymer and therefore exhibited amorphous structure, with only a
378 broad peak at $2\theta=15^\circ$ - 27° .⁵³ Since there are no crystalline peaks of NaCl in AZF, NaCl is likely no
379 longer present as a crystalline compound in this fiber, likely being converted into an amorphous
380 state during electrospinning process due to the large elongational force and rapid evaporation of
381 the solvent that may confound crystallization.^{54,55}

382 Chemical characterization was carried out by FTIR (Figure 2f). FTIR spectra of ZF and
383 AZF exhibited peaks at 1653 cm^{-1} and 1540 cm^{-1} , corresponding to the amide I and amide II of
384 C=O stretching of the zein structure.⁵³ The presence of each of the AIs in AZF was also evident
385 from the spectra. First, thyme oil exhibited peaks at 3500 - 3300 cm^{-1} , 1627 cm^{-1} , 1360 cm^{-1} , 1250
386 cm^{-1} , and 800 cm^{-1} , due to the OH stretching, aromatic C=C stretching, isopropyl group, C-O
387 stretching, and aromatic C-H bending vibrations.⁵⁶ The peak observed at 1250 cm^{-1} in the spectra
388 of AZF may belong to C-O stretching vibration of thyme oil.⁵⁶ Secondly, citric acid has its
389 characteristic peaks at 3290 cm^{-1} , 1721 cm^{-1} , 1105 cm^{-1} , and 778 cm^{-1} , belonging to the O-H
390 stretching, C=O stretching, C-OH stretching, and CH_2 rocking, respectively. Therefore, the peak
391 in the spectra of AZF at 1721 cm^{-1} may be attributed to C=O stretching of citric acid.⁵⁷ Lastly, the
392 peaks observed in the spectra of AZF at 1653 cm^{-1} and 1540 cm^{-1} , which were attributed to the
393 amide groups, showed the presence of nisin in AZF.^{58,59} However, the extremely low levels of AIs
394 incorporated into the chemical structure of the fibers results to weak signals for those AI in the

1
2
3 395 FTIR spectra making it difficult to distinguish from the stronger polymer signal (The fibers consists
4
5 396 of 90% biopolymer). In the FTIR spectra of AZF, the C-O stretching vibration of thyme oil at 1250
6
7 397 cm^{-1} , C=O stretching of citric acid at 1721 cm^{-1} , and amide groups of nisin at 1653 cm^{-1} and 1540
8
9 398 cm^{-1} were identified indicative of the incorporation of AIs. Finally, the dissolution kinetics of AIs
10
11 399 under simulant conditions presented in Figures 4a-b are also confirming the presence of AIs in a
12
13 400 more quantifiable manner.

14
15
16
17 401 **Development of antimicrobial active ingredient (AI) cocktail:** Figure S2-S4 summarizes
18
19 402 the antimicrobial activity of single AIs (thyme oil, citric acid and nisin) and their combinations at
20
21 403 a range of concentrations against *E. coli* and *L. innocua* using the disk diffusion test. Five % (w/v)
22
23 404 thyme oil was effective against both *E. coli* and *L. innocua*, showing a zone of inhibition of ~10
24
25 405 mm. Nisin, which was dissolved in 1% (w/v) citric acid because of its poor solubility at neutral pH,
26
27 406 was effective against *L. innocua* (zone of inhibition of ~8 mm) but not against *E. coli*. This is not
28
29 407 surprising as nisin is known to be effective against gram-positive bacteria by forming pores on cell
30
31 408 membrane and disrupting cell wall synthesis.^{32,60} On the other hand, the liposaccharide in the outer
32
33 409 membrane of gram-negative bacteria protects them from nisin activity.^{42,60}

34
35
36
37 410 The cocktail of 5% (w/v) thyme oil, 1% (w/v) citric acid and 0.005% (w/v) nisin exhibited
38
39 411 the greatest antimicrobial activity against both *E. coli* and *L. innocua*, showing a zone of inhibition
40
41 412 of ~10 mm (Figure S2-S4). However, the strong odor of thyme oil in this cocktail will most likely
42
43 413 have a negative impact on the organoleptic properties of food. The cocktail of 1% (w/v) thyme oil,
44
45 414 5% (w/v) citric acid and 0.005% (w/v) nisin showed zones of inhibition of ~9 mm for *E. coli* and
46
47 415 ~8 mm for *L. innocua*. Therefore, this cocktail, which showed equivalent antimicrobial effects but
48
49 416 contains less thyme oil, was chosen for further studies.

1
2
3 417 It is worth noting that synergistic antimicrobial effects of AIs has been shown previously in
4
5 418 studies by the authors and others.^{61,62} Zhou et al. (2007) showed that neither thymol nor citric acid
6
7 419 inhibited the growth of *Salmonella* Typhimurium, whereas their combination reduced *Salmonella*
8
9 420 after 24 hours by 2.8 log.⁶¹ Zhao et al. (2017) showed that nisin did not inhibit the growth of *Listeria*
10
11 421 *monocytogenes* and that citric acid only reduced *Listeria monocytogenes* by ~1.5 log after 10 hours;
12
13 422 however, their combination reduced *Listeria* by more than 5 log of after 10 hours.⁶²
14
15

16
17 423 **Assessment of antimicrobial efficacy of zein fibers:** Pristine zein fibers (ZF) slightly
18
19 424 enhanced the growth of *E. coli* by ~1.5 log in 24 hours (Figure 3a); there was no impact on the
20
21 425 growth of *L. innocua* (Figure 3b). A possible explanation is that *E. coli* can release extracellular
22
23 426 protease and breakdown zein, a protein, in the fiber and thereby release amino acids to support
24
25 427 growth. A previous study confirmed that the *E. coli* strain (ATCC 25922) exhibited extracellular
26
27 428 protease activity.⁶³
28
29

30
31 429 Antimicrobial zein fibers (AZF) reduced *E. coli* by 3.0 log and 4.7 log at 1 hour and 24
32
33 430 hours, respectively (Figure 3a). For *L. innocua* (Figure 3b), the reduction caused by AZF was 4.9
34
35 431 log (close to the detection limit) at both 1 hour and 24 hours. Notably, at the 1-hour contact time,
36
37 432 the antimicrobial efficacy of AZF against *E. coli* was lower than the case of *L. innocua*. This is
38
39 433 likely due to presence of nisin in the cocktail, which is particularly effective against gram-positive
40
41 434 bacteria.³²
42
43

44
45 435 Aluminum foil coated with the AI cocktail was used as a comparator sample for the
46
47 436 antimicrobial efficacy test. After 1 hour and 24 hours of contact, *E. coli* was reduced by 4.7 log by
48
49 437 this comparator sample, in contrast to 3.0 and 4.7 log by AZF, respectively (Figure 3a). The
50
51 438 inactivation of *L. innocua* was 4.9 log after 1 hour and 24 hours of contact for both the comparator
52
53 439 sample and AZF (Figure 3b). It is worth noting that the comparator sample has more than an order
54
55

1
2
3 440 of magnitude greater AI loading (3.63 mg of AI/cm²) than AZF (0.250 mg of AI/cm²). Importantly,
4
5 441 the antimicrobial efficacy of AZF after 24 hours of contact was equivalent to the comparator
6
7 442 sample. This finding is consistent with the previous studies demonstrating that electrospun fibers
8
9 443 showed significantly greater antimicrobial activity than traditional films with similar loadings of
10
11 444 antimicrobials.^{64,65} As noted above, the unique property of electrospun fibers over AI-infused films
12
13 445 is their higher surface-to-volume-ratio, enabling nearly all of the AIs to be on the surface and
14
15 446 thereby yielding similar antimicrobial efficacy at much lower AI amount.
16
17
18

19 447 The antimicrobial efficacy of AZF against *P. italicum* was also evaluated. AZF did not show
20
21 448 inactivation effect against *P. italicum* spores (Figure S3-S5). This is likely due to the greater
22
23 449 resistance of fungal spores to antimicrobial agents or perhaps to the loading used; a greater AI
24
25 450 loading amount may have yielded control.⁶⁶
26
27

28 451 In comparison to previous studies with other biopolymer-based fibers, AZF exhibits similar
29
30 452 or greater antimicrobial efficacies against *E. coli* and *L. innocua* (~5 log reduction in 24 hours).
31
32 453 Lin et al. (2018) showed that electrospun thyme oil/gelatin fibers could inhibit the growth of
33
34 454 *Campylobacter jejuni* on chicken by ~1-2 log in 24 hours.⁶⁷ Similarly, Lin et al. (2019) reported
35
36 455 that electrospun thyme oil/silk fibroin fibers could reduce *Salmonella typhimurium* on chicken and
37
38 456 duck meat by ~1-4 log in 24 hours.⁶⁸ Aytac et al. (2017) reported that electrospun zein fibers
39
40 457 incorporated with thymol, which is the main component of thyme oil, inhibited the growth of *E.*
41
42 458 *coli* and *Staphylococcus aureus* in suspension by ~55% and 67% in 24 hours, respectively.²¹
43
44
45

46 459 In addition, as shown in Figure 3a, when the mass per surface area of AZF decreased from
47
48 460 2.50 mg/cm² to 1.25 mg/cm², the efficacy of *E. coli* inactivation was reduced significantly ($P <$
49
50 461 0.05) from 3.0 to 2.2 log at a contact time of 1 hour. At 24 hours contact time, no significant
51
52 462 difference ($P > 0.05$) of *E. coli* inactivation was found between the two AI loadings (Figure 3a).
53
54
55

1
2
3 463 For *L. innocua*, the antimicrobial efficacy of AZF reached the detection limit in 1 hour for both AI
4
5 464 loading levels; there was no significant difference in efficacy between the fibers (Figure 3b).

6
7 465 The antimicrobial efficacy of AZFs after storage at 4°C for 4 weeks was unchanged against
8
9 466 *E. coli* at 1 hour and 24 hours of contact (Figure 3a). However, AZF showed slightly reduced
10
11 467 inactivation efficiency against *L. innocua* after 4 weeks of storage, with 3.4-log reduction in 1 hour
12
13 468 compared to 4.9-log reduction prior to storage. It is worth noting that the 4-week storage of the
14
15 469 AZF did not affect the 24-hour contact time activity (4.9-log reduction) (Figure 3b). Lower efficacy
16
17 470 against *L. innocua* could be due to the loss in nisin activity over time.⁶⁹ Wu et al. (2018) also found
18
19 471 that nisin-anchored cellulose film showed less antimicrobial efficacy against a gram-positive
20
21 472 bacterium, *Alicyclobacillus acidoterrestris*, after a 3-month storage period.⁷⁰ It is also possible that
22
23 473 evaporation of thyme oil occurred over time, which was previously reported as a limitation for the
24
25 474 use of essential oils.⁷¹

26
27
28
29
30 475 **AI release kinetics from zein fibers in various food simulants:** The cumulative release
31
32 476 (%) of AIs from AZFs into the selected food simulants over a 240-hour period is shown in Figure
33
34 477 4a-b. The loading efficiency (LE) values, which are the percentage (%) of AIs successfully loaded
35
36 478 in the AZFs, were determined as 60% and 57% for thymol and nisin, respectively; these values
37
38 479 were used to calculate the percent AI release. As shown in Figure 4a, AZF exhibited a rapid release
39
40 480 of thymol in all media, with complete dissolution in 2 hours. Small diameter of fibers results to
41
42 481 both high specific surface area (SSA) and surface to volume ratio compared to films. This high
43
44 482 SSA results to AIs to be mostly located on the surface of the fiber making them more bioactive
45
46 483 when pathogens get in contact with such surfaces.⁷² In addition, hydrophilic amino acids in the zein
47
48 484 structure facilitated fiber wettability and AI solubility.⁴³ It is also worth noting that AZF completely
49
50 485 dissolved in 50% ethanol and this may have also caused the highest thymol release, along with high
51
52
53
54
55

1
2
3 486 solubility of thymol, in this medium.⁷³ Lastly, the release of thymol was higher in 3% acetic acid
4
5 487 than water due to higher solubility in acidic medium.⁷⁴ Nisin release profiles from AZF varied and
6
7 488 were also dependent on the medium as shown in Figure 4b. Nisin release was relatively slow in 3%
8
9 489 acetic acid compared to water; thus, the release was completed in 12 hours in 3% acetic acid versus
10
11 490 6 hours in water. In addition, the release of nisin in 3% acetic acid was slightly greater than its
12
13 491 release in water. This result can be explained by the higher solubility of nisin in 3% acetic acid as
14
15 492 compared to water.
16
17
18

19 493 The use of miniscule amounts of AIs in the structure of AZF results to miniscule quantities
20
21 494 of AIs released in food simulants and as a result not only the microorganisms will be eliminated in
22
23 495 contact but potential sensory effects such as taste change, discoloration, etc. will be minimum and
24
25 496 less than those of using same AIs in films. It is also worth noting that the AIs used here are non-
26
27 497 toxic and classified as safe by US FDA. Finally, in future studies, detailed sensory assessment
28
29 498 based on the type of food to be stored using such fibers will be performed.
30
31
32

33 499 **Scalability of fiber synthesis using a multi-needle injector:** Electrospun fibers have a
34
35 500 great potential to be used in industrial applications; therefore, it is also important to demonstrate
36
37 501 scalability of the proposed synthesis by using a multi-needle injector as described in the method
38
39 502 section. It is worth noting that recent advances on electrospinning and development of multi-needle
40
41 503 injector enabled scaling up the process and used in biomedical applications.²³ As illustrated in this
42
43 504 study, the use of a 20-needle injector enabled us to increase the fiber production yield to 1 g/h
44
45 505 which shows that the approach can be scaled up and commercialized and used by the food
46
47 506 packaging industry. Here, the operational parameters such as flow rate, applied voltage, and needle-
48
49 507 collector distance, are of great importance for the uniform distribution of the electric field
50
51 508 throughout the needles.^{23,75} The optimized parameters for the multi-needle synthesis were adjusted
52
53
54
55

1
2
3 509 and found to be 3 mL/h, 35 kV (27.5 kV was applied to the needle; -7.5 kV was applied to the
4
5 510 collector), and 15 cm for flow rate, applied voltage, and needle-collector distance, respectively

6
7 511 Figure S4a-S6 shows the SEM image of AZF synthesized using these optimized
8
9
10 512 electrospinning parameters. The fibers are bead-free and uniform; the diameter distribution graph
11
12 513 is given in Figure S4b-S6 and shows values up to 400 nm, with an average diameter of 160 ± 40 nm.
13
14 514 Importantly, this is quite similar to the average diameter of AZF (165 ± 35 nm) synthesized by
15
16 515 single-needle injector (Figure 2d). It is also worth mentioning that the yield for AZF synthesized
17
18 516 by single and multi-needle injectors were calculated to be 0.12 g/h and 1 g/h, respectively. In
19
20 517 conclusion, these results showed fiber synthesis scalability, which is important for industrial and
21
22 518 food sector applications. It is worth noting that while electrospinning can be scaled up and used in
23
24 519 the production of fibers from biopolymers for food packaging, the cost might be prohibitive for
25
26 520 some food applications. On the other hand, the use of biodegradable biopolymers will reduce the
27
28 521 environmental footprint and more importantly consumers expressed willingness to pay more for
29
30 522 those biodegradable materials.^{76,77,78}

31
32
33 523 **Preliminary assessment of fibers affinity to attach to the substrates:** Since fiber
34
35 524 detachment from the AZF surface could confound efficacy, hydraulic pressure was applied to the
36
37 525 fibers to improve the affinity to the substrate. SEM images of the pressure-applied AZFs
38
39 526 synthesized on aluminum foil are shown in Figure S5a-c-S7. Here, various pressure and time
40
41 527 combinations were utilized: 3 MPa for 2 and 4 min, and 12 MPa for 2 min. When the lowest
42
43 528 pressure (3 MPa) (Figure S5a-b-S7) was used, the AZF porosity was slightly decreased.⁷⁹ The
44
45 529 difference in fiber porosity was minimal when the pressure was applied for 2 minutes compared to
46
47 530 4 min. In addition to the change in porosity, applying 12 MPa for 2 minutes also resulted in an
48
49 531 overt bunching at certain locations (Figure S5c-S7). Visual observation of fibers showed that an

1
2
3 532 application of 3 MPa pressure applied for 4 minutes was the optimum condition to increase fiber
4
5 533 affinity to the surface.
6

7
8 534 In order to evaluate fiber affinity to the substrate (aluminum foil), a 200 g weight was
9
10 535 applied for 5 minutes and then removed in order to evaluate fiber detachment. Some of the fibers
11
12 536 detached from the surface for non-pressure applied fibers, whereas no fiber detached for the
13
14 537 hydraulically pressured fibers (3 MPa for 4 min). These results demonstrate that it is possible to
15
16
17 538 coat substrates with fibers that remain intact even after exposure to forces typical of food packaging
18
19 539 conditions applied.
20

21 540 **CONCLUSIONS**

22
23
24 541 Designing bio-degradable packaging materials has become an area of great interest in the
25
26 542 food industry, particularly given that the excess use of synthetic polymers is causing environmental
27
28 543 concerns due to the release of micro-/nanoplastics. In addition, the incorporation of antimicrobials
29
30 544 into the package is an effective way to enhance food safety and quality while promoting
31
32 545 sustainability. Here, a scalable, green, and one-step synthesis approach was developed to synthesize
33
34 546 antimicrobial zein fibers containing an AI cocktail composed of nature-derived FDA-classified
35
36
37 547 Generally Recognized as Safe (GRAS) antimicrobials having different mechanisms of action.
38
39 548 These antimicrobial fibers are suitable for use in food packaging materials to enhance food safety
40
41 549 and quality. Scalability of the platform was also demonstrated using a multi-needle injector system.
42
43
44 550 Finally, the developed fibers were able to efficiently inactivate broad-spectrum of food-associated
45
46 551 microorganisms, with reductions of ~5 logs for *E. coli* and *L. innocua* after 24 hours of contact.
47
48 552 Additionally, antimicrobial activity at 24-hour contact time was retained after 4 weeks of material
49
50
51 553 storage at 4°C. Further studies are underway to explore sensory evaluation tests such as color,
52
53
54 554 texture, and taste of food that was stored in fiber-containing packaging materials.
55

555 **ACKNOWLEDGEMENTS**

556 This research is supported by the Nanyang Technological University-Harvard T. H. Chan
557 School of Public Health Initiative for Sustainable Nanotechnology (Project No: NTU-HSPH
558 18003). We would like to acknowledge Zhenyuan Zhang for his assistance in carrying out XRD
559 analysis. This work was performed in part at the Center for Nanoscale Systems (CNS), a member
560 of the National Nanotechnology Coordinated Infrastructure Network (NNCI), which is supported
561 by the National Science Foundation under NSF award no. 1541959. CNS is part of Harvard
562 University.

563 **SUPPORTING INFORMATION**

564 The Supporting Information is available free of charge on the ACS Publications website:
565 <http://pubs.acs.org>.

- 566 -SEM images of beaded fibers
- 567 -Table showing the surface area analysis of fibers
- 568 -Antimicrobial activity of single and combined AIs
- 569 - Antimicrobial activity of fibers against *P. Italicum*
- 570 - SEM image of fibers synthesized by a multi-needle injector
- 571 - SEM images of fibers after applying pressure

572 **REFERENCES**

- 573 (1) Willett, W.; Rockström, J.; Loken, B.; Springmann, M.; Lang, T.; Vermeulen, S.; Garnett,
574 T.; Tilman, D.; Declerck, F. The Lancet Commissions Food in the Anthropocene : The
575 EAT – Lancet Commission on Healthy Diets from Sustainable Food Systems. *Lancet*
576 **2019**, *393* (10170), 447–492, DOI 10.1016/S0140-6736(18)31788-4.
- 577 (2) World Health Organization (WHO). WHO Estimates of the Global Burden of Foodborne

- 1
2
3 578 Diseases: Foodborne Disease Burden Epidemiology Reference Group 2007-2015
4
5 579 <https://apps.who.int/iris/handle/10665/199350> (accessed July 10, 2020).
6
7
8 580 (3) Scallan, E.; Hoekstra, R. M.; Angulo, F. J.; Tauxe, R. V; Widdowson, M.; Roy, S. L.;
9
10 581 Jones, J. L.; Griffin, P. M. Foodborne Illness Acquired in the United States — Major
11
12 582 Pathogens. *Emerg. Infect. Dis.* **2011**, *17* (1), 1–21, DOI 10.3201/eid1701.P11101.
13
14 583 (4) Hoffmann, S.; Macculloch, B.; Batz, M. Economic Burden of Major Foodborne Illnesses
15
16 584 Acquired in the United States (No. 1476-2016-120935).
17
18 585 (5) USDA, United States Department of Agriculture. Food Waste FAQs
19
20 586 <https://www.usda.gov/foodwaste/faqs> (accessed July 10, 2020).
21
22
23 587 (6) Cole, M. B.; Augustin, M. A.; Robertson, M. J.; Manners, J. M. The Science of Food
24
25 588 Security. *npj Sci. Food* **2018**, *2* (1), 1–8, DOI 10.1038/s41538-018-0021-9.
26
27 589 (7) Mlalila, N.; Kadam, D. M.; Swai, H.; Hilonga, A. Transformation of Food Packaging from
28
29 590 Passive to Innovative via Nanotechnology : Concepts and Critiques. *J. Food Sci. Technol.*
30
31 591 **2016**, *53* (9), 3395–3407, DOI 10.1007/s13197-016-2325-6.
32
33 592 (8) Han, Jia-wei; Luis. Ruiz-Garcia; Jian-Ping, Qian; Xin-Ting, Y. Food Packaging : A
34
35 593 Comprehensive Review and Future Trends. *Food Sci. Food Saf.* **2018**, *17* (4), 860–877,
36
37 594 DOI 10.1111/1541-4337.12343.
38
39 595 (9) Siracusa, V.; Rocculi, P.; Romani, S.; Rosa, M. D. Biodegradable Polymers for Food
40
41 596 Packaging: A Review. *Trends Food Sci. Technol.* **2008**, *19* (12), 634–643, DOI
42
43 597 10.1016/j.tifs.2008.07.003.
44
45 598 (10) Cox, K. D.; Covernton, G. A.; Davies, H. L.; Dower, J. F.; Juanes, F.; Dudas, S. E. Human
46
47 599 Consumption of Microplastics. *Environ. Sci. Technol.* **2019**, *53* (12), 7068–7074, DOI
48
49 600 10.1021/acs.est.9b01517.
50
51
52
53
54
55

- 1
2
3 601 (11) OECD. Improving Plastics Management : Trends , Policy Responses , and the Role of
4
5 602 International Co-Operation and Trade. *Environ. Policy Pap.* **2018**, No. 12, 20 (accessed
6
7 603 July 10, 2020).
- 8
9
10 604 (12) Ajay, S. M.; Lalit, Y.; Dash, M. B. S. K.; Mahanti, N. K. Application of Biodegradable
11
12 605 Polymers in Food Packaging Industry : A Comprehensive Review. *J. Packag. Technol.*
13
14 606 *Res.* **2018**, 3 (1), 77–96, DOI 10.1007/s41783-018-0049-y.
- 15
16
17 607 (13) Yu, Z.; Rao, G.; Wei, Y.; Yu, J.; Wu, S.; Fang, Y. Preparation, Characterization, and
18
19 608 Antibacterial Properties of Biofilms Comprising Chitosan and ϵ -Polylysine. *Int. J. Biol.*
20
21 609 *Macromol.* **2019**, 141, 545–552, DOI 10.1016/j.ijbiomac.2019.09.035.
- 22
23
24 610 (14) Pranoto, Y.; Rakshit, S. K. Ā.; Salokhe, V. M. Enhancing Antimicrobial Activity of
25
26 611 Chitosan Films by Incorporating Garlic Oil , Potassium Sorbate and Nisin. *Food Sci.*
27
28 612 *Technol.* **2005**, 38 (8), 859–865. DOI 10.1016/j.lwt.2004.09.014.
- 29
30
31 613 (15) Malhotra, B.; Keshwani, A.; Kharkwal, H. Antimicrobial Food Packaging: Potential and
32
33 614 Pitfalls. *Front. Microbiol.* **2015**, 6, 611, DOI 10.3389/fmicb.2015.00611.
- 34
35
36 615 (16) Senthil Muthu Kumar, T.; Senthil Kumar, K.; Rajini, N.; Siengchin, S.; Ayrilmis, N.;
37
38 616 Varada Rajulu, A. A Comprehensive Review of Electrospun Nanofibers: Food and
39
40 617 Packaging Perspective. *Compos. Part B Eng.* **2019**, 175, 107074, DOI
41
42 618 10.1016/j.compositesb.2019.107074.
- 43
44
45 619 (17) Rodrigues, S. M.; Demokritou, P.; Dokoozlian, N.; Hendren, C. O.; Karn, D. B.; Mauter,
46
47 620 M. S.; Sadik, O. A.; Safarpour, M.; Unrine, J. M.; Viers, J.; Welle, P.; White, J. C.; De, M.
48
49 621 R. W.; Lowry, G. V. Nanotechnology for Sustainable Food Production : Promising
50
51 622 Opportunities and Scientific Challenges. *Environ. Sci. Nano* **2017**, 4 (4), 767–781, DOI
52
53 623 10.1039/c6en00573j.

- 1
2
3 624 (18) Eleftheriadou, M.; Pyrgiotakis, G.; Demokritou, P. Nanotechnology to the Rescue : Using
4
5 625 Nano-Enabled Approaches in Microbiological Food Safety and Quality. *Curr. Opin.*
6
7 626 *Biotechnol.* **2017**, *44*, 87–93, DOI 10.1016/j.copbio.2016.11.012.
8
9
10 627 (19) Kumar, V.; Elfving, A.; Koivula, H.; Bous, D.; Toivakka, M. Roll-to-Roll Processed
11
12 628 Cellulose Nano Fiber Coatings. *Ind. Eng. Chem. Res.* **2016**, *55* (12), 3603–3613, DOI
13
14 629 10.1021/acs.iecr.6b00417.
15
16
17 630 (20) Altan, A.; Aytac, Z.; Uyar, T. Carvacrol Loaded Electrospun Fibrous Films from Zein and
18
19 631 Poly(Lactic Acid) for Active Food Packaging. *Food Hydrocoll.* **2018**, *81*, 48–59, DOI
20
21 632 10.1016/j.foodhyd.2018.02.028.
22
23
24 633 (21) Aytac, Z.; Ipek, S.; Durgun, E.; Tekinay, T.; Uyar, T. Antibacterial Electrospun Zein
25
26 634 Nanofibrous Web Encapsulating Thymol/Cyclodextrin-Inclusion Complex for Food
27
28 635 Packaging. *Food Chem.* **2017**, *233*, 117–124, DOI 10.1016/j.foodchem.2017.04.095.
29
30
31 636 (22) Soto, K. M.; Loarca-piña, G.; Luna-bárceñas, G.; Mendoza, S. Antimicrobial Effect of
32
33 637 Nisin Electrospun Amaranth : Pullulan Nanofibers in Apple Juice and Fresh Cheese. *Int. J.*
34
35 638 *Food Microbiol.* **2019**, *295*, 25–32, DOI 10.1016/j.ijfoodmicro.2019.02.001.
36
37
38 639 (23) Xue, J.; Wu, T.; Dai, Y.; Xia, Y.; States, U. Electrospinning and Electrospun Nanofibers :
39
40 640 Methods, Materials, and Applications. *Chem. Rev.* **2019**, *119* (8), 5298–5415, DOI
41
42 641 10.1021/acs.chemrev.8b00593.
43
44
45 642 (24) Vaze, N.; Pyrgiotakis, G.; Mena, L.; Baumann, R.; Demokritou, A.; Ericsson, M.; Zhang,
46
47 643 Y.; Bello, D.; Eleftheriadou, M.; Demokritou, P. A Nano-Carrier Platform for the Targeted
48
49 644 Delivery of Nature-Inspired Antimicrobials Using Engineered Water Nanostructures for
50
51 645 Food Safety Applications. *Food Control* **2019**, *96*, 365–374, DOI
52
53 646 10.1016/j.foodcont.2018.09.037.
54
55

- 1
2
3 647 (25) Huang, R.; Vaze, N.; Soorneedi, A.; Moore, M. D.; Xue, Y.; Bello, D.; Demokritou, P.
4
5 648 Inactivation of Hand Hygiene-Related Pathogens Using Engineered Water Nanostructures.
6
7 649 *ACS Sustain. Chem. Eng.* 2019, 7 (24), 19761–19769, DOI
8
9 10.1021/acssuschemeng.9b05057.
10 650
11
12 651 (26) Li, D.; Xia, Y. Electrospinning of Nanofibers: Reinventing the Wheel? *Adv. Mater.* 2004,
13
14 652 16 (14), 1151–1170, DOI 10.1002/adma.200400719.
15
16
17 653 (27) Mohammad, S.; Mousavi, M.; Afra, E.; Tajvidi, M.; Bousfield, D. W. Application of
18
19 654 Cellulose Nanofibril (CNF) as Coating on Paperboard at Moderate Solids Content and
20
21 655 High Coating Speed Using Blade Coater. *Prog. Org. Coatings* 2018, 122, 207–218, DOI
22
23 10.1016/j.porgcoat.2018.05.024.
24 656
25
26 657 (28) Mousavi, S. M. M.; Afra, E.; Tajvidi, M.; Bousfield, D. W. Cellulose
27
28 658 Nanofiber/Carboxymethyl Cellulose Blends as an Efficient Coating to Improve the
29
30 659 Structure and Barrier Properties of Paperboard. *Cellulose* 2017, 24 (7), 3001–3014, DOI
31
32 10.1007/s10570-017-1299-5.
33 660
34
35 661 (29) Khaneghah, A. M.; Mohammad, S.; Hashemi, B.; Es, I.; Fracassetti, D.; Limbo, S.
36
37 662 Efficacy of Antimicrobial Agents for Food Contact Applications : Biological Activity,
38
39 663 Incorporation into Packaging, and Assessment Methods : A Review. *J. Food Protec* 2018,
40
41 664 81 (7), 1142–1156, DOI 10.4315/0362-028XJFP-17-509.
42
43
44 665 (30) Melo, D.; Ribeiro-santos, R.; Andrade, M. Use of Essential Oils in Active Food
45
46 666 Packaging : Recent Advances and Future Trends. *Trends Food Sci. Technol.* 2017, 61,
47
48 667 132–140, DOI 10.1016/j.tifs.2016.11.021.
49
50
51 668 (31) Tariq, S.; Wani, S.; Rasool, W.; Shafi, K.; Ahmad, M.; Prabhakar, A.; Hussain, A.; Rather,
52
53 669 M. A. A Comprehensive Review of the Antibacterial, Antifungal and Antiviral Potential of

- 1
2
3 670 Essential Oils and Their Chemical Constituents against Drug-Resistant Microbial
4
5 671 Pathogens. *Microb. Pathog.* **2019**, *134*, 103580, DOI 10.1016/j.micpath.2019.103580.
6
7
8 672 (32) Irkin, R.; Esmer, O. K. Novel Food Packaging Systems with Natural Antimicrobial
9
10 673 Agents. *J. Food Sci. Technol.* **2015**, *52* (10), 6095–6111, DOI 10.1007/s13197-015-1780-
11
12 674 9.
13
14 675 (33) Theron, M. M.; Lues, J. A. N. F. R. Organic Acids and Meat Preservation : A Review.
15
16 676 *Food Rev. Int.* **2007**, *23* (2), 141–158, DOI 10.1080/87559120701224964.
17
18
19 677 (34) Cieplik, F.; Kara, E.; Muehler, D.; Enax, J.; Hiller, K. A.; Maisch, T.; Buchalla, W.
20
21 678 Antimicrobial Efficacy of Alternative Compounds for Use in Oral Care toward Biofilms
22
23 679 from Caries-Associated Bacteria in Vitro. *Microbiologyopen* **2019**, *8* (4), e00695, DOI
24
25 680 10.1002/mbo3.695.
26
27
28 681 (35) Park, S.; Choi, M.; Park, J.; Park, K.; Chung, M.; Ryu, S.; Kang, D. Use of Organic Acids
29
30 682 to Inactivate Escherichia Coli Monocytogenes on Organic Fresh Apples and Lettuce. *J.*
31
32 683 *Food Sci.* **2011**, *76* (6), M293–M298, DOI 10.1111/j.1750-3841.2011.02205.x.
33
34
35 684 (36) Sagong, H.; Lee, S.; Chang, P.; Heu, S.; Ryu, S.; Choi, Y.; Kang, D. Combined Effect of
36
37 685 Ultrasound and Organic Acids to Reduce Escherichia Coli O157 : H7, Salmonella
38
39 686 Typhimurium, and Listeria Monocytogenes on Organic Fresh Lettuce. *Int. J. Food*
40
41 687 *Microbiol.* **2011**, *145* (1), 287–292, DOI 10.1016/j.ijfoodmicro.2011.01.010.
42
43
44 688 (37) Buck, A. K.; Elmore, D. E.; Darling, L. E. O. Using Fluorescence Microscopy to Shed
45
46 689 Light on the Mechanisms of Antimicrobial Peptides. *Future Med. Chem.* **2019**, *11* (18),
47
48 690 2447–2460, DOI 10.4155/fmc-2019-0095.
49
50
51 691 (38) Hudzicki, J. Kirby-Bauer Disk Diffusion Susceptibility Test Protocol. *Am. Soc. Microbiol.*
52
53 692 **2009**, *12*, 1–23.
54
55

- 1
2
3 693 (39) ASTM. Standard Test Method for Determining the Activity of Incorporated Antimicrobial
4
5 694 Agent(s) In Polymeric or Hydrophobic Materials <https://www.astm.org/Standards/E2180>
6
7 695 (accessed July 10, 2020).
8
9
10 696 (40) Gündüz, G. T.; Pazir, F. Inactivation of *Penicillium Digitatum* and *Penicillium Italicum*
11
12 697 under in Vitro and in Vivo Conditions by Using UV-C Light. *J. Food Prot.* **2013**, *76* (10),
13
14 698 1761–1766, DOI 10.4315/0362-028X.JFP-12-511.
15
16
17 699 (41) FDA. Guidance for Industry: Preparation of Premarket Submissions for Food Contact
18
19 700 Substances (Chemistry Recommendations) <https://www.fda.gov/regulatory->
20
21 701 [information/search-fda-guidance-documents/guidance-industry-preparation-premarket-](https://www.fda.gov/regulatory-information/search-fda-guidance-documents/guidance-industry-preparation-premarket-)
22
23 702 [submissions-food-contact-substances-chemistry](https://www.fda.gov/regulatory-information/search-fda-guidance-documents/guidance-industry-preparation-premarket-submissions-food-contact-substances-chemistry) (accessed July 10, 2020).
24
25
26 703 (42) Gharsallaoui, A.; Joly, C.; Oulahal, N.; Degraeve, P.; Lyon, U. De; Lyon, U.; Lyon, I.;
27
28 704 Biodymia, L. Nisin as a Food Preservative: Part 2: Antimicrobial Polymer Materials
29
30 705 Containing Nisin. *Crit. Rev. Food Sci. Nutr.* **2013**, *56* (8), 1275–1289, DOI
31
32 706 10.1080/10408398.2013.763766.
33
34
35 707 (43) Kasaai, M. R. Zein and Zein -Based Nano-Materials for Food and Nutrition Applications:
36
37 708 A Review. *Trends Food Sci. Technol.* **2018**, *79*, 184–197, DOI 10.1016/j.tifs.2018.07.015.
38
39
40 709 (44) Uyar, T.; Besenbacher, F. Electrospinning of Uniform Polystyrene Fibers: The Effect of
41
42 710 Solvent Conductivity. *Polymer.* **2008**, *49* (24), 5336–5343, DOI
43
44 711 10.1016/j.polymer.2008.09.025.
45
46
47 712 (45) Luo, C. J.; Nangrejo, M.; Edirisinghe, M. A Novel Method of Selecting Solvents for
48
49 713 Polymer Electrospinning. *Polymer.* **2010**, *51* (7), 1654–1662, DOI
50
51 714 10.1016/j.polymer.2010.01.031.
52
53
54 715 (46) Wannatong, L.; Sirivat, A.; Supaphol, P. Effects of Solvents on Electrospun Polymeric
55

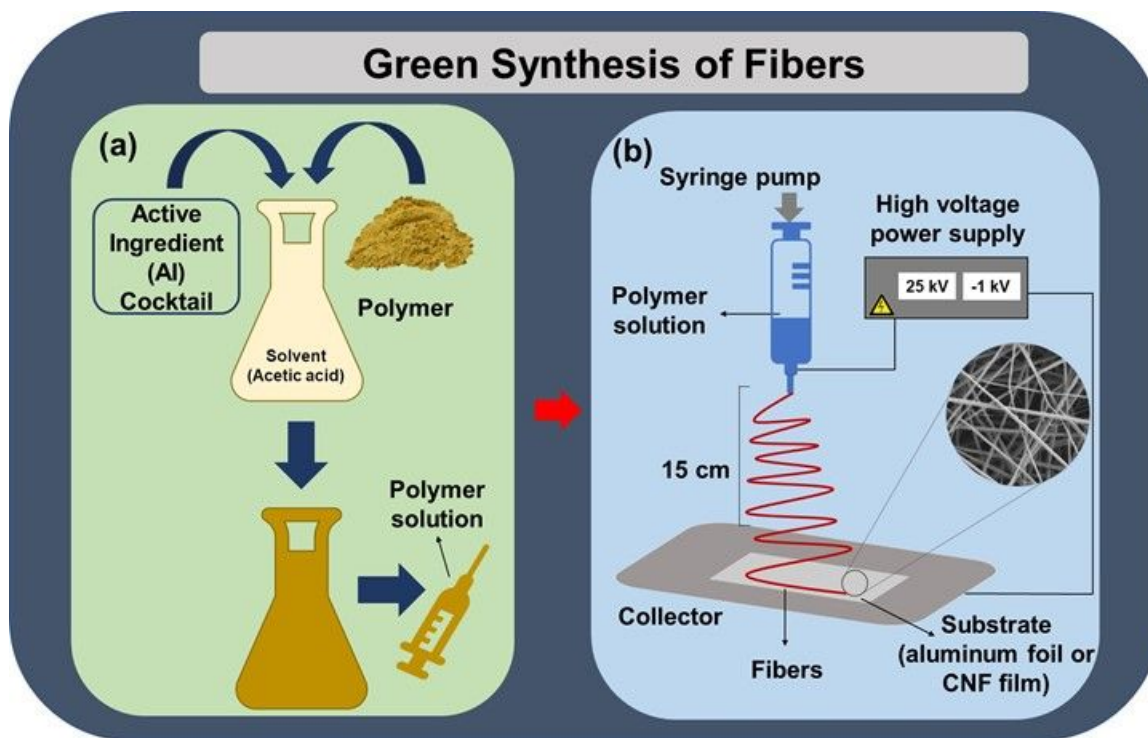
- 1
2
3 716 Fibers : Preliminary Study on Polystyrene. *Polym. Int.* **2004**, *53* (11), 1851–1859, DOI
4
5 717 10.1002/pi.1599.
6
7
8 718 (47) Selling, G. W.; Biswas, A.; Patel, A.; Walls, D. J.; Dunlap, C.; Wei, Y. Impact of Solvent
9
10 719 on Electrospinning of Zein and Analysis of Resulting Fibers. *Macromol. Chem. Phys.*
11
12 720 **2007**, *208* (9), 1002–1010, DOI 10.1002/macp.200700056.
13
14 721 (48) Burdock, G. A.; Carabin, I. G. Generally Recognized as Safe (GRAS): History and
15
16 722 Description. *Toxicol. Lett.* **2004**, *150* (1), 3–18, DOI 10.1016/j.toxlet.2003.07.004.
17
18
19 723 (49) Shenoy, S. L.; Bates, W. D.; Frisch, H. L.; Wnek, G. E. Role of Chain Entanglements on
20
21 724 Fiber Formation during Electrospinning of Polymer Solutions: Good Solvent, Non-
22
23 725 Specific Polymer-Polymer Interaction Limit. *Polymer.* **2005**, *46* (10), 3372–3384, DOI
24
25 726 10.1016/j.polymer.2005.03.011.
26
27
28 727 (50) Roya M. Nezarati, Michelle B. Eifert, E. C.-H. Effects of Humidity and Solution Viscosity
29
30 728 on Electrospun Fiber Morphology. *Tissue Eng. Part C Methods* **2013**, *19* (10), 810–819,
31
32 729 DOI 10.1089/ten.tec.2012.0671.
33
34
35 730 (51) Nthumbi, R. M.; Ngila, J. C. Electrospun and Functionalized PVDF/PAN Nanocatalyst-
36
37 731 Loaded Composite for Dechlorination and Photodegradation of Pesticides in Contaminated
38
39 732 Water. *Environ. Sci. Pollut. Res.* **2016**, *23* (20), 20214–20231, DOI 10.1007/s11356-016-
40
41 733 7136-9.
42
43
44 734 (52) Zheng, X.; Con, C. O. S. N. Effects of Chitosan Oligosaccharide – Nisin Conjugates
45
46 735 Formed by Maillard Reaction on the Preservation of *Collichthys Niveatus*. *J. Food*
47
48 736 *Process. Preserv.* **2019**, *43* (10), e14116, DOI 10.1093/fqsafe/fyz016.
49
50
51 737 (53) Kayaci, F.; Uyar, T. Electrospun Zein Nanofibers Incorporating Cyclodextrins. *Carbohydr.*
52
53 738 *Polym.* **2012**, *90* (1), 558–568, DOI 10.1016/j.carbpol.2012.05.078.
54
55

- 1
2
3 739 (54) Aytac, Z.; Sen, H. S.; Durgun, E.; Uyar, T. Sulfisoxazole/Cyclodextrin Inclusion Complex
4
5 740 Incorporated in Electrospun Hydroxypropyl Cellulose Nanofibers as Drug Delivery
6
7 741 System. *Colloids Surfaces B Biointerfaces* **2015**, *128*, 331–338, DOI
8
9 742 10.1016/j.colsurfb.2015.02.019.
10
11
12 743 (55) Brennan, D. A.; Conte, A. A.; Kanski, G.; Turkula, S.; Hu, X.; Kleiner, M. T.; Beachley,
13
14 744 V. Mechanical Considerations for Electrospun Nanofibers in Tendon and Ligament Repair.
15
16 745 *Adv. Healthc. Mater.* **2018**, *7* (12), 1701277, DOI 10.1002/adhm.201701277.
17
18
19 746 (56) Trindade, G. G. G.; Thirvikraman, G.; Menezes, P. P.; França, C. M.; Lima, B. S.;
20
21 747 Carvalho, Y. M. B. G.; Souza, E. P. B. S. S.; Duarte, M. C.; Shanmugam, S.; Quintans-
22
23 748 júnior, L. J.; Bezerra, D. P.; Bertassoni, L. E.; Araújo, A. A. S. Carvacrol/ β -Cyclodextrin
24
25 749 Inclusion Complex Inhibits Cell Proliferation and Migration of Prostate Cancer Cells.
26
27 750 *Food Chem. Toxicol.* **2019**, *125*, 198–209, DOI 10.1016/j.fct.2019.01.003.
28
29
30 751 (57) Pimpang, P.; Sumang, R.; Choopun, S. Effect of Concentration of Citric Acid on Size and
31
32 752 Optical Properties of Fluorescence Graphene Quantum Dots Prepared by Tuning
33
34 753 Carbonization Degree. *J. Sci.* **2018**, *45*, 2005–2014.
35
36
37 754 (58) Song, Z.; Yuan, Y.; Niu, C.; Dai, L.; Wei, J.; Yue, T. Iron Oxide Nanoparticles
38
39 755 Functionalized with Nisin for Rapid Inhibition and Separation of: *Alicyclobacillus* Spp.
40
41 756 *RSC Adv.* **2017**, *7* (11), 6712–6719, DOI 10.1039/C6RA25860C.
42
43
44 757 (59) Niaz, T.; Shabbir, S.; Noor, T.; Abbasi, R.; Raza, Z. A. Polyelectrolyte Multicomponent
45
46 758 Colloidosomes Loaded with Nisin Z for Enhanced Antimicrobial Activity against
47
48 759 Foodborne Resistant Pathogens. *Front. Microbiol.* **2018**, *8*, 2700, DOI
49
50 760 10.3389/fmicb.2017.02700.
51
52
53 761 (60) Juncioni, L.; Arauz, D.; Faustino, A.; Vessoni, T. C. Nisin Biotechnological Production
54
55

- 1
2
3 762 and Application : A Review. *Trends Food Sci. Technol.* **2009**, *20* (3–4), 146–154, DOI
4
5 763 10.1016/j.tifs.2009.01.056.
6
7
8 764 (61) Zhou, F., Ji, B., Zhang, H., Jiang, H., Yang, Z., Li, J., ... & Yan, W. Synergistic Effect of
9
10 765 Thymol and Carvacrol Combined with Chelators and Organic Acids against Salmonella
11
12 766 Typhimurium. *J. Food Prot.* **2007**, *70* (7), 1704–1709, DOI 10.4315/0362-028X-
13
14 767 70.7.1704.
15
16
17 768 (62) Zhao, X.; Zhen, Z.; Wang, X.; Guo, N. Synergy of a Combination of Nisin and Citric Acid
18
19 769 against Staphylococcus Aureus and Listeria Monocytogenes. *Food Addit. Contam. - Part A*
20
21 770 *Chem. Anal. Control. Expo. Risk Assess.* **2017**, *34* (12), 2058–2068, DOI
22
23 771 10.1080/19440049.2017.1366076.
24
25
26 772 (63) Adesegun, S. A.; Samuel, O. F.; Anthony, B. O.; Folasade, B. O.; Mary, S. K. Essential
27
28 773 Oil of Syzygium Samarangense ; A Potent Antimicrobial and Inhibitor of Partially Purified
29
30 774 and Characterized Extracellular Protease of Escherichia Coli 25922. *Br. J. Pharmacol.*
31
32 775 *Toxicol.* **2013**, *4* (6), 215–221, DOI 10.19026/bjpt.4.5405.
33
34
35 776 (64) Wen, P.; Zhu, D. H.; Feng, K.; Liu, F. J.; Lou, W. Y.; Li, N.; Zong, M. H.; Wu, H.
36
37 777 Fabrication of Electrospun Polylactic Acid Nanofilm Incorporating Cinnamon Essential
38
39 778 Oil/ β -Cyclodextrin Inclusion Complex for Antimicrobial Packaging. *Food Chem.* **2016**,
40
41 779 *196*, 996–1004, DOI 10.1016/j.foodchem.2015.10.043.
42
43
44 780 (65) Wen, P.; Zhu, D. H.; Wu, H.; Zong, M. H.; Jing, Y. R.; Han, S. Y. Encapsulation of
45
46 781 Cinnamon Essential Oil in Electrospun Nanofibrous Film for Active Food Packaging.
47
48 782 *Food Control* **2016**, *59*, 366–376, DOI 10.1016/j.foodcont.2015.06.005.
49
50
51 783 (66) Marchese, A.; Orhan, I. E.; Daglia, M.; Barbieri, R.; Lorenzo, D.; Nabavi, S. F.; Gortzi,
52
53 784 O.; Izadi, M.; Mohammad, S. Antibacterial and Antifungal Activities of Thymol: A Brief

- 1
2
3 785 Review of the Literature. *Food Chem.* **2016**, *210*, 402–414, DOI
4
5 786 10.1016/j.foodchem.2016.04.111.
6
7
8 787 (67) Lin, L.; Zhu, Y.; Cui, H. LWT - Food Science and Technology Electrospun Thyme
9
10 788 Essential Oil / Gelatin Nanofibers for Active Packaging against *Campylobacter Jejuni* in
11
12 789 Chicken. *LWT - Food Sci. Technol.* **2018**, *97*, 711–718, DOI 10.1016/j.lwt.2018.08.015.
13
14 790 (68) Lin, L.; Liao, X.; Cui, H. Cold Plasma Treated Thyme Essential Oil/Silk Fibroin Nano Fi
15
16 791 bers against *Salmonella Typhimurium* in Poultry Meat. *Food Packag. Shelf Life* **2019**, *21*,
17
18 792 100337, DOI 10.1016/j.fpsl.2019.100337.
19
20
21 793 (69) Rollema, H. S.; Kuipers, O. P.; Both, P.; Willem, M.; Siezen, R. J. Improvement of
22
23 794 Solubility and Stability of the Antimicrobial Peptide Nisin by Protein Engineering. *Appl.*
24
25 795 *Environ. Microbiol.* **1995**, *61* (8), 2873–2878.
26
27
28 796 (70) Wu, H.; Teng, C.; Liu, B.; Tian, H.; Wang, J. Characterization and Long Term
29
30 797 Antimicrobial Activity of the Nisin Anchored Cellulose Films. *Int. J. Biol. Macromol.*
31
32 798 **2018**, *113*, 487–493, DOI 10.1016/j.ijbiomac.2018.01.194.
33
34
35 799 (71) Luo, M.; Cao, Y.; Wang, W.; Chen, X.; Cai, J.; Wang, L.; Xiao, J. Sustained-Release
36
37 800 Antimicrobial Gelatin Film: Effect of Chia Mucilage on Physicochemical and
38
39 801 Antimicrobial Properties. *Food Hydrocoll.* **2018**, *87*, 783–791, DOI
40
41 802 <https://doi.org/10.1016/j.foodhyd.2018.09.010>.
42
43
44 803 (72) Li, X.; Kanjwal, M. A.; Lin, L.; Chronakis, I. S. Electrospun Polyvinyl-Alcohol
45
46 804 Nanofibers as Oral Fast-Dissolving Delivery System of Caffeine and Riboflavin. *Colloids*
47
48 805 *Surfaces B Biointerfaces* **2013**, *103*, 182–188, DOI 10.1016/j.colsurfb.2012.10.016.
49
50
51 806 (73) Azar Aghamohammadi, Mohammad Azadbakht, S. J. H. Quantification of Thymol
52
53 807 Content in Different Extracts of *Zataria Multiflora* by HPLC Method. *Pharm. Biomed. Res.*

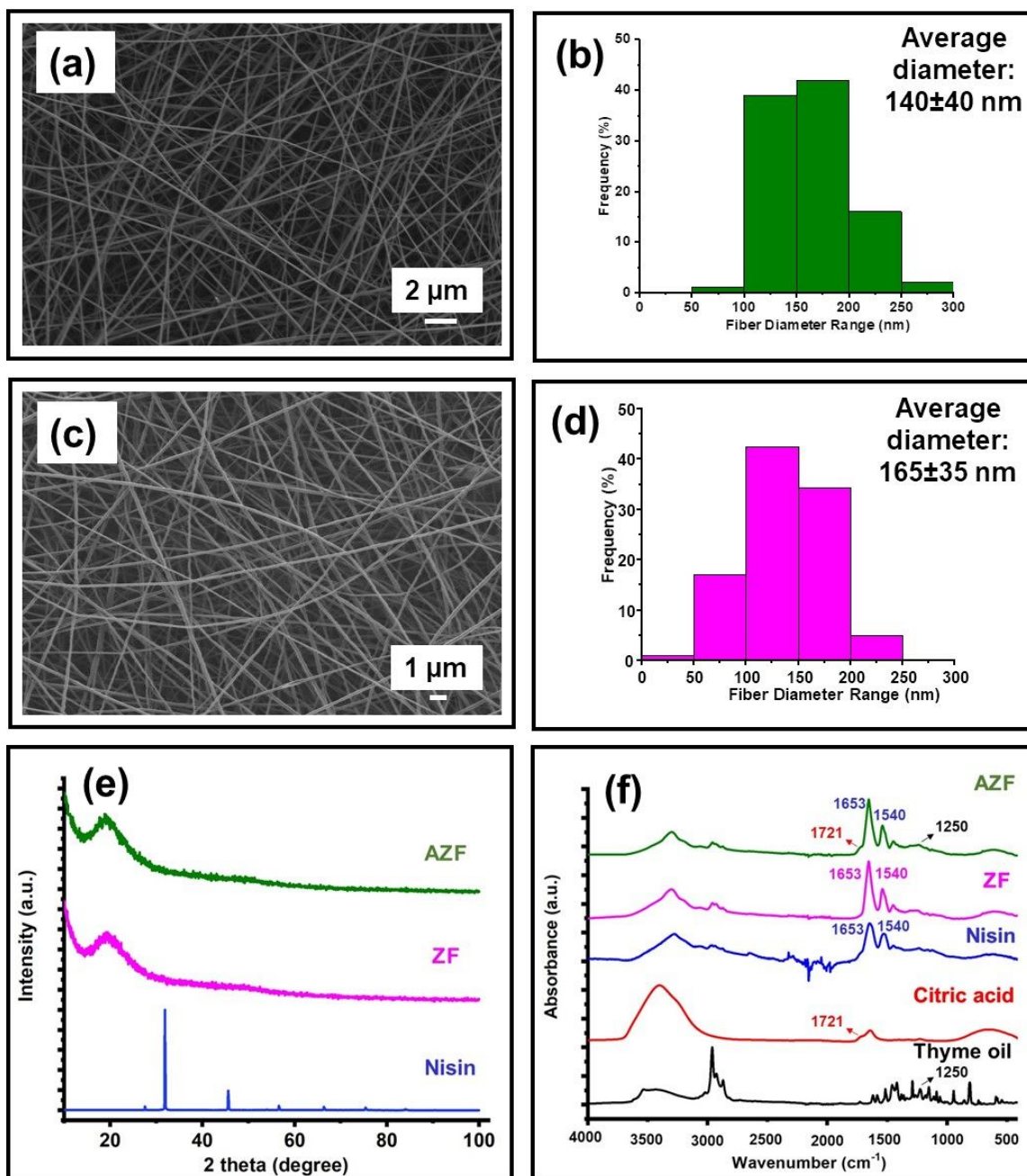
- 1
2
3 808 **2016**, 2 (1), 8–13, DOI 10.18869/acadpub.pbr.2.1.8.
4
5 809 (74) Amariei, G.; Boltes, K.; Leto, P.; Iriepa, I. Poly (Amidoamine) Dendrimers Grafted on
6
7 810 Electrospun Poly (Acrylic Acid)/Poly (Vinyl Alcohol) Membranes for Host–Guest
8
9 811 Encapsulation of Antioxidant Thymol. *J. Mater. Chem. B* **2017**, 5 (33), 6776–6785, DOI
10
11 812 10.1039/C7TB01498H.
12
13
14 813 (75) Salehuddin, H. S.; Mohamad, E. N.; Nur, W.; Mahadi, L. Multiple-Jet Electrospinning
15
16 814 Methods for Nanofiber Processing : A Review Multiple-Jet Electrospinning Methods for
17
18 815 Nanofiber Processing : A Review. *Mater. Manuf. Process.* **2017**, 33 (5), 479–498, DOI
19
20 816 10.1080/10426914.2017.1388523.
21
22
23 817 (76) Dilkes-Hoffman, L.; Ashworth, P.; Laycock, B.; Pratt, S.; Lant, P. Public Attitudes
24
25 818 towards Bioplastics – Knowledge , Perception and End-of-Life Management. *Resour.*
26
27 819 *Conserv. Recycl.* **2019**, 151 (June), 104479, DOI 10.1016/j.resconrec.2019.104479.
28
29
30 820 (77) Herbes, C.; Beuthner, C.; Ramme, I. Consumer Attitudes towards Biobased Packaging e A
31
32 821 Cross-Cultural Comparative Study. *J. Clean. Prod.* **2018**, 194, 203–218, DOI 10.
33
34 822 1016/j.jclepro.2018.05.106.
35
36
37 823 (78) Yue, C.; Hall, C. R.; Behe, B. K.; Campbell, B. L.; Lopez, R. G.; Dennis, J. H.
38
39 824 Investigating Consumer Preference for Biodegradable Containers. **2010**, 28 (December),
40
41 825 239–243, DOI 10.24266/0738-2898-28.4.239.
42
43
44 826 (79) Wang, Z.; Crandall, C.; Sahadevan, R.; Menkhaus, T. J. Micro Filtration Performance of
45
46 827 Electrospun Nano Fiber Membranes with Varied Fiber Diameters and Different Membrane
47
48 828 Porosities and Thicknesses. *Polymer.* **2017**, 114, 64–72, DOI
49
50 829 10.1016/j.polymer.2017.02.084.
51
52
53
54 830



831

832 **Figure 1.** Schematic representation of (a) the preparation of active ingredient (AI) cocktail that is
833 loaded into the polymer solution and (b) the synthesis of fibers incorporated with AI cocktail by
834 electrospinning.

835



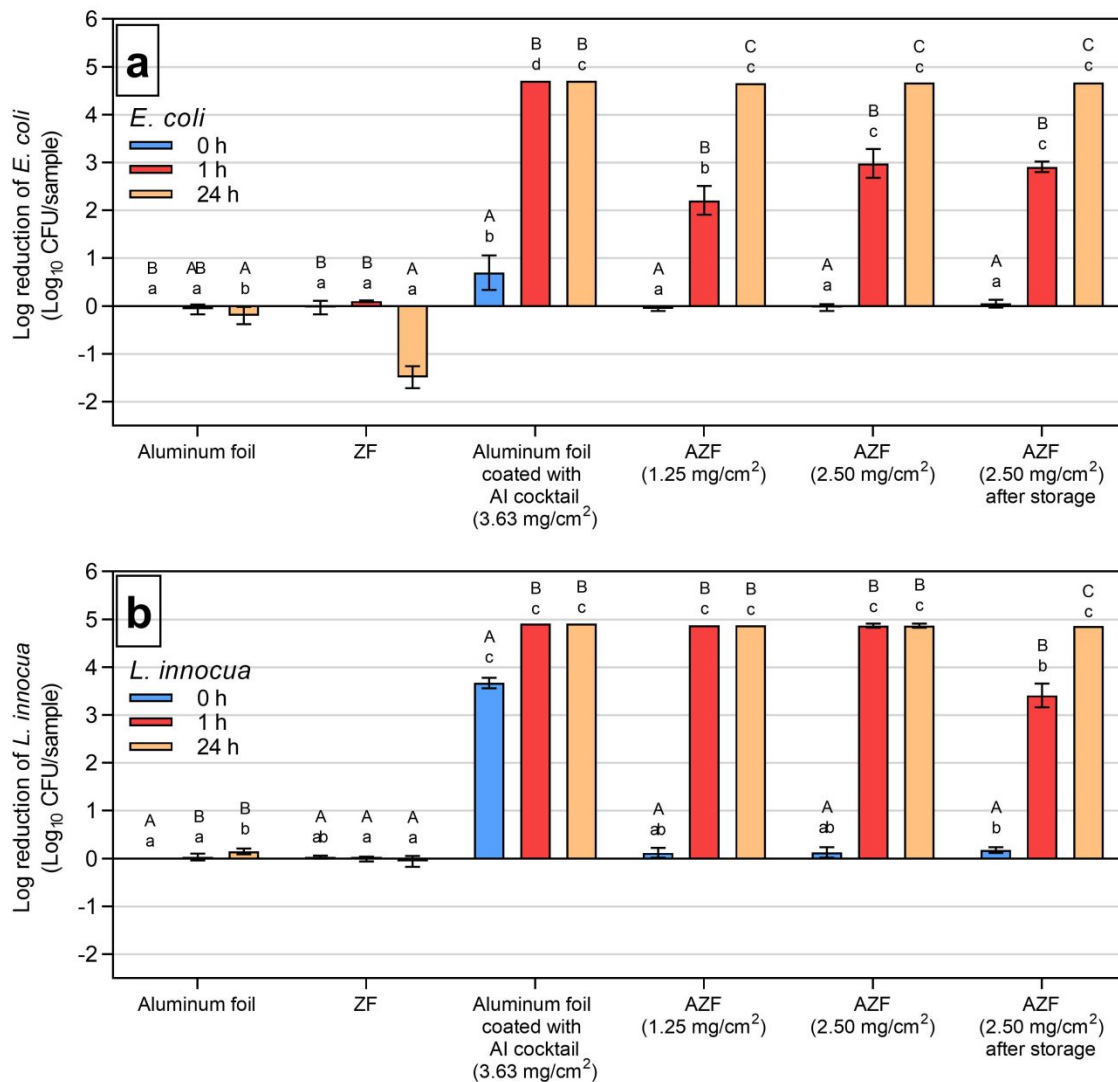
836

837 **Figure 2.** Scanning electron microscopy (SEM) images and fiber diameter distribution graphs of
838 (a,b) ZF and (c,d) AZF; (e) X-Ray diffraction (XRD) patterns of nisin, ZF, and AZF; and (f) Fourier
839 transform infrared spectrometer (FTIR) spectra of thyme oil, citric acid, nisin, ZF, and AZF.

840

841

842



843

844 **Figure 3.** The antimicrobial activity of aluminum foil, zein fibers (ZF), aluminum foil coated with
 845 active ingredient (AI) cocktail, antimicrobial zein fibers (AZF) (1.25 mg/cm²), AZF (2.50 mg/cm²),
 846 AZF after storage at 4°C for 4 weeks against (a) *E. coli* and (b) *L. innocua*. Data in the same material
 847 group labeled with the same uppercase letter are not significantly different ($P > 0.05$). Data in the
 848 same treatment time group labeled with the same lowercase letter are not significantly different (P
 849 > 0.05).

850

851

852

853

854

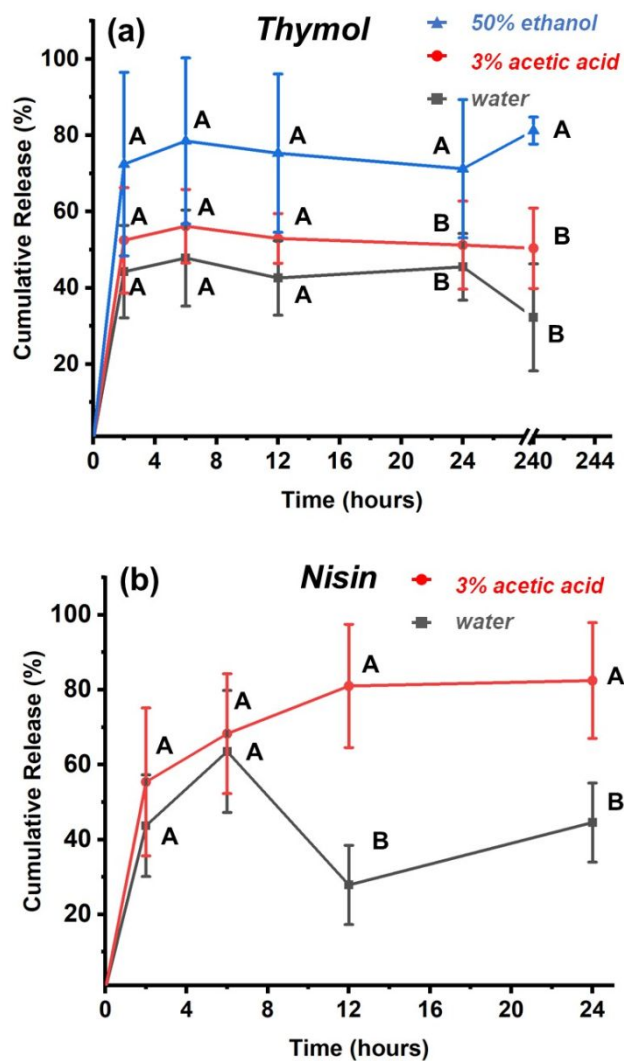


Figure 4. The cumulative release (%) of (a) thymol and (b) nisin from antimicrobial zein fibers (AZF) into food simulants as a function of time. (a) Values at a specific time point that have a different letter are significantly different (One-way ANOVA with a Holm-Sidak multiple comparison test at $p < 0.05$). * = significantly different at $p = 0.066$. (b) Values at a specific time point that have a different letter are significantly different (Student t-test; $p < 0.05$).

1
2
3 866 **For Table of Contents use only**
4
5

